BIOCHEMISTRY
including biophysical chemistry & molecular biology

Article

pubs.acs.org/biochemistry

Efficient Isolation of *Pseudomonas aeruginosa* Type III Secretion Translocators and Assembly of Heteromeric Transmembrane Pores in Model Membranes

Fabian B. Romano,[∥,⊥] Kyle C. Rossi,[∥] Christos G. Savva,[†] Andreas Holzenburg,[†,‡,§] Eugenia M. Clerico,[∥] and Alejandro P. Heuck*[,∥,⊥]

[†]Microscopy and Imaging Center, [‡]Department of Biology, and [§]Department of Biochemistry and Biophysics, Texas A&M University, College Station, Texas 77843, United States

[∥]Department of Biochemistry and Molecular Biology and [⊥]Program in Molecular and Cellular Biology, University of Massachusetts, Amherst, Massachusetts 01003, United States

Supporting Information

ABSTRACT: Translocation of bacterial toxins or effectors into host cells using the type III secretion (T3S) system is a conserved mechanism shared by many Gram-negative pathogens. *Pseudomonas aeruginosa* injects different proteins across the plasma membrane of target cells, altering the normal metabolism of the host. Protein translocation presumably occurs through a proteinaceous transmembrane pore formed by two T3S secreted protein translocators, PopB and PopD. Unfolded translocators are secreted through the T3S needle prior to insertion into the target membrane. Purified PopB and PopD form pores in model membranes. However, their tendency to form heterogeneous aggregates in solution had hampered the analysis of how these proteins undergo the transition from a denatured state to a membrane-inserted state. Translocators were purified as stable complexes with the cognate chaperone PcrH and isolated from the chaperone using 6 M urea. We report here the assembly of stable transmembrane pores by dilution of urea-denatured translocators in the presence of membranes. PopB and PopD spontaneously bound liposomes containing anionic phospholipids and cholesterol in a pH-dependent manner as observed by two independent assays, time-resolved Förster resonance energy transfer and sucrose-step gradient ultracentrifugation. Using Bodipy-labeled proteins, we found that PopB interacts with PopD on the membrane surface as determined by excitation energy migration and fluorescence quenching. Stable transmembrane pores are more efficiently assembled at pH <5.0, suggesting that acidic residues might be involved in the initial membrane binding and/or insertion. Altogether, the experimental setup described here represents an efficient method for the reconstitution and analysis of membrane-inserted translocators.

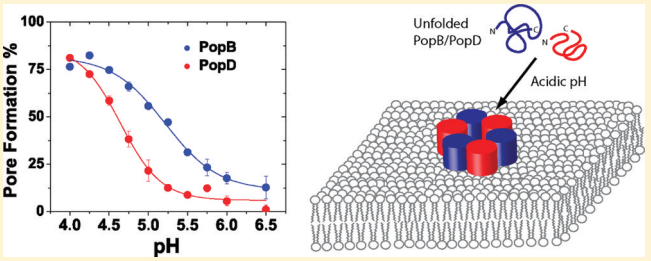

Transport of proteins across membranes is essential at many stages of pathogen infection and colonization of human cells. This process is important for discharging the proteins outside the pathogenic organism (secretion) and for introduction of these secreted toxins and effectors into the cytosol of the target cell (translocation). Many pathogens, including *Shigella*, *Salmonella*, *Yersinia*, and *Pseudomonas* species, exploit a sophisticated and efficient mechanism of toxin secretion and translocation known as the type III secretion (T3S) system.[1−3] It is well-known that *Pseudomonas aeruginosa* pathogenesis depends on a vast arsenal of virulence factors, including the T3S system, which is a key factor for acute infections.[4,5] The T3S system is a syringelike macromolecular secretion system formed by more than 20 different proteins organized into three major structures to span (i) the inner bacterial membrane, the periplasmic space, and the outer bacterial membrane (secreton); (ii) the extracellular space (needle); and (iii) the host cellular membrane (translocon). Great progress has been made in the structural characterization of the secreton and the needle in related organisms.[6] However, virtually nothing is known about how T3S-secreted proteins are translocated across the plasma membrane of the target cell.[7] Some genetic and biochemical evidence suggests that effector proteins are translocated across the host plasma membrane through a proteinaceous pore or translocon formed by two bacterially secreted proteins (the translocon hypothesis).[7−9]

The translocon hypothesis states that the *P. aeruginosa* T3S translocators, PopB and PopD, insert into the target membrane, engage with the tip of the T3S needle (formed by PcrV[10]), and assist in the translocation of effector proteins into the host cell. The hypothesis is based on the following experimental observations. (i) PcrV, PopB, and PopD are not required for effector secretion but are essential for translocation of the effector into the target cell.[11−13] (ii) Only PopB and PopD are

Received: June 11, 2011
Revised: July 16, 2011
Published: July 19, 2011

found inserted into the target membrane after pathogen−host contact.[13] (iii) PcrV, PopB, and PopD are necessary for the observation of T3S-dependent cell lysis.[11,13,14] (iv) PopB and PopD can form pores in model membranes either individually or in combination.[15,16]

Current models for the *P. aeruginosa* translocon complex are quite rudimentary, and they are based on the following observations. (i) Translocon proteins PopB and PopD are found associated with cell membranes after the interaction of *P. aeruginosa* with red blood cells.[13] (ii) PopB co-immunoprecipitates with PopD after Triton X-100 solubilization of membrane-associated proteins.[13] (iii) Ringlike structures are observed using electron microscopy when the translocon proteins are incubated with model membranes.[15] The topology of the translocon proteins is based only on the bioinformatic analysis of the primary structure for these proteins, which suggests that PopB possesses two potential transmembrane (TM) segments and PopD only one,[8] but no experimental data are available to corroborate such predictions. The nonpolar character of the T3S translocators and their tendency to aggregate in solution have made the structural and functional characterization of these proteins very difficult.[17,18]

We have purified and characterized the *P. aeruginosa* translocators individually as homogeneous complexes with the cognate chaperone PcrH. After isolation, PopB and PopD were quantitatively separated from PcrH by combining immobilized metal ion affinity chromatography (IMAC) and elution with the chaotropic agent urea. The spectroscopic characterization of the urea-isolated PopD showed little secondary structure content and the fact that the two Trp residues were exposed to a polar environment. In contrast, the urea-isolated PopB exhibited greater α-helical content than PopD, and its single Trp residue was located in a nonpolar environment. The pore forming activity of the urea-isolated translocators was very similar to the activity of the translocators separated from the chaperone by acidification.[16] Assembly and maximal pore formation occurred at pH <5, indicating that protonation of acidic residues was critical for membrane insertion. Under these conditions, PopD, PopB, and their mixtures formed discrete and stable pores in lipid vesicles. Cryo-electron microscopy (EM) and dynamic light scattering (DLS) revealed that no aggregation or disruption of the integrity of the vesicles occurred after assembly of the transmembrane pores. Single Cys residues were introduced at specific locations in PopD and PopB, and these derivatives purified and labeled with the fluorescent probe Bodipy. Using both Bodipy excitation energy migration and self-quenching, we unambiguously showed that PopB interacts with PopD on lipid membranes. We have therefore established an efficient procedure for purifying, specifically labeling, and assembling the *P. aeruginosa* translocators and their derivatives into model membranes.

EXPERIMENTAL PROCEDURES

Expression and Purification of Proteins. The expression and purification of hisPcrH, the hisPcrH−PopD complex, the hisPcrH−PopB complex, and their derivatives were conducted as described in the Supporting Information. The protein concentration was estimated using molar absorptivities of 18910 M^{-1} cm^{-1} for hisPcrH, 13980 M^{-1} cm^{-1} for PopD, and 6990 M^{-1} cm^{-1} for PopB,[19] and assuming 1:1 chaperone−translocator complexes.

Isolation of PopB and PopD Using 6 M Urea. Purified hisPcrH-PopD [or hisPcrH-PopB (2−4 mg)] was loaded onto spinTrap IMAC columns (GE Healthcare) packed with 300 μL each of Quelating Sepharose Fast Flow (GE Healthcare) resin slurry, previously loaded with Co^{2+} and equilibrated with buffer A [20 mM 2-amino-2-(hydroxymethyl)propane-1,3-diol (Tris-HCl) (pH 8.0) and 100 mM NaCl]. Dissociation of PopB or PopD from hisPcrH was achieved when the columns were spun dry for 30 s at 2000*g*; 450 μL of buffer B [20 mM Tris-HCl (pH 8.0)] supplemented with 6 M urea and 20 mM Gly was added, and the columns were incubated for 30 min at 4 °C on a rocking platform. Dissociated PopD (or PopB) was eluted when the columns were spun for 30 s at 2000*g*. Samples were fractionated, frozen in liquid N_2, and stored at −80 °C until they were used.

Mass Spectrometry. Purified PopB and PopD were analyzed using an Esquire Mass spectrometer (Bruker Daltonics, Billerica, MA) equipped with an electrospray ionization source and ion-trap mass detector; 0.1 mg of protein was dialyzed extensively against pure water at 4 °C. Then, protein was diluted to 50% (v/v) methanol and 3% acetic acid and sprayed intro the ionization source at a rate of 120 μL/h. Mass/charge data were collected and averaged, and the protein molecular mass was calculated from deconvolution of the average mass spectra.

Fluorescent Protein Labeling. $PopB^{S164C}$ (introduced mutations are indicated using a superscript in which the substituted amino acid and the introduced amino acid are given to the left and right of the number, respectively) and $PopD^{F223C}$ were labeled using *N*-[(4,4-difluoro-5,7-dimethyl-4-bora-3a,4a-diaza-*s*-indacen-3-yl)methyl]iodoacetamide (Bodipy FL C_1-IA or Bodipy, Invitrogen) as follows. Two milligrams of $PopB^{S164C}$ or $PopD^{F223C}$ complexed with hisPcrH were first incubated in buffer A supplemented with 5 mM DTT for 1 h and then run through a Sephadex G-25 column (1.5 cm inside diameter × 20 cm) pre-equilibrated with buffer C [50 mM Hepes (pH 8.0) and 100 mM NaCl]. Given the relatively low water solubility of Bodipy, dye dissolved in dimethyl sulfoxide was added in four consecutive steps to the protein solution with a 5:1 dye:protein ratio. The first two additions were followed by incubation for 1 h at 20−23 °C in the dark with gentle shaking, while the last two additions were followed by a 30 min incubation under the same conditions. Then, any precipitated dye and protein were cleared out by centrifugation, and excess soluble fluorophore was removed by SEC using Sephadex G-25 resin pre-equilibrated with 20 mM Tris (pH 7.5) and 100 mM NaCl. $PopB^{S164C-Bodipy}$ and $PopD^{F223C-Bodipy}$ were isolated from hisPcrH using 6 M urea as described for wild-type translocators. The nonlytic, prepore former Perfringolysin O derivative ($PFO^{E167C/F181A/F318A/C459A}$ or PFO) was labeled with Bodipy as indicated above for the translocators. Labeling efficiencies were calculated to be 96% for $PopD^{F223C-Bodipy}$, 68% for $PopB^{S164C-Bodipy}$, and 100% for PFO^{Bodipy} using the molar absorptivities at 280 nm for PopB and PopD (see above), PFO,[20] and Bodipy (55000 cm^{-1} M^{-1} at 502 nm in 6 M urea). The absorbance of Bodipy at 280 nm was ~4% of the absorbance at 502 nm.

Liposome Preparation. All non-sterol lipids were obtained from Avanti Polar Lipids (Alabaster, AL). Cholesterol was obtained from Steraloids (Newport, RI). Liposomes were generated using an Avanti (Alabaster, AL) Mini-Extruder and polycarbonate filters with a 0.1 μm pore size (Whatman) as described previously.[21] Briefly, a mixture of 1-palmitoyl-2-oleoyl-*sn*-glycero-3-phosphocholine (POPC), cholesterol, and

1-palmitoyl-2-oleoyl-*sn*-glycero-3-phosphoserine (POPS) (in a molar ratio of 65:20:15) in chloroform was dried at 20−23 °C under N_2 and then kept under vacuum for at least 3 h. Lipids were hydrated via addition of buffer C to a final concentration of total lipids of 10−30 mM and incubated for 30 min at 20−23 °C with vortexing at 5 min intervals. The suspended phospholipid/sterol mixture was frozen in liquid N_2 and thawed at 37 °C a total of three cycles to reduce the number of multilamellar liposomes and to enhance the trapped volumes of the vesicles. Hydrated lipids were extruded 21 times through a 0.1 μm pore size polycarbonate filter. All liposome preparations were analyzed as monodisperse with an average particle diameter of ∼100 ± 5 nm using DLS. The resultant liposomes were stored at 4 °C and used within 2 weeks of production. Liposomes used in Förster resonance energy transfer (FRET) experiments were prepared similarly, except that 0.5 mol % total lipid was replaced with rhodamine B 1,2-dihexadecanoyl-*sn*-glycero-3-phosphoethanolamine (Rh-PE), triethylammonium salt (Invitrogen). The pore forming activity of translocators was measured using liposomes containing $Tb(DPA)_3^{3-}$. The liposomes loaded with $Tb(DPA)_3^{3-}$ were prepared as described previously by us.[22]

Liposome Flotation−Membrane Binding Assay. Binding reaction mixtures (75 μL) containing liposomes (2 mM total lipids) and Bodipy-labeled PopB or PopD (400 nM total protein) were established in ultracentrifuge tubes and incubated at 20−23 °C for 1 h. Binding reaction buffer was a mixture of 30 mM sodium acetate and 30 mM 2-(*N*-morpholino)-ethanesulfonic acid regulated at pH 4.0 or 6.0. Liposomes were equilibrated with the buffer prior to the addition of protein. Liposome-bound and unbound proteins were separated by flotation of proteoliposomes through a sucrose gradient as follows. A 225 μL aliquot of 67% sucrose was thoroughly mixed with each binding reaction mixture, and the samples were overlaid with 360 μL of 40% sucrose, followed by 240 μL of 4% sucrose. Samples were centrifuged for 50 min at 90000*g* and 4 °C.[23] Three 300 μL fractions (upper fraction containing proteoliposomes, middle fraction empty, and bottom fraction containing free protein) were collected from the gradient. After trichloroacetic acid precipitation and resuspension in SDS denaturalization buffer, samples were analyzed by SDS−PAGE followed by a fluorescence scan using a FLA-500 phosphorimager (Fujifilm Corp.). Protein bands corresponding to liposome-bound protein were quantified by gel densitometry using Genetools version 4.01 (Syngene).

Dynamic Light Scattering. Unless otherwise indicated, the average size of the liposomes was determined at 20−23 °C using a PDDLS Coolbatch/PD2000DLS instrument (Precision Detectors, Inc., Franklin, MA) employing a 30 mW He−Ne laser source (658 nm) and a photodiode detector at an angle of 90°. Average autocorrelation functions were fit using the cumulant method and hydrodynamic radius derived from the obtained decay rates.[24]

Cryo-EM. Samples were prepared for cryo-EM via application of 3 μL of the liposome/protein mixture to freshly glow-discharged holey carbon films (C-Flat, Protochips Inc.) and plunge-frozen in liquid ethane using a FEI Vitrobot. Specimens were observed on an FEI Tecnai F20 transmission electron microscope operating at 200 kV. Images were acquired under low-dose and zero-loss imaging conditions on a Gatan Ultrascan 1000 CCD camera attached to the end of a Gatan Tridiem postcolumn energy filter.

Pore Formation Assay. Liposomes were suspended at a final total lipid concentration of 0.15−0.30 mM in 300 μL of buffer D [50 mM sodium acetate (pH 4.0) and 5 mM EDTA]. The net initial emission intensity (F_0) was determined after equilibration of the sample at 25 °C for 5 min. Aliquots of PopB or PopD were added to the liposome suspension at concentrations of 30−60 nM, and samples were incubated for 15 min at ∼23 °C. After re-equilibration to 25 °C, the final net emission intensity (F_f) of the sample was determined (i.e., after blank subtraction and dilution correction) and the fraction of $Tb(DPA)_3^{3-}$ quenched was estimated using $(F_0 - F_f)/F_0$.[22] For the analysis of the pore forming activity at different pH values, an equimolar mixture of 30 mM sodium acetate and 30 mM 2-(*N*-morpholino)ethanesulfonic acid was used.

Analysis of Formed Pores. The presence of discrete size membrane pores formed by PopB, PopD, or an additive equimolar mixture of both was assessed by measuring the ability of biocytin (∼1.5 nm size) or biotin-β-amylase (∼4 nm size) to diffuse through the pores formed by the translocators. Liposomes encapsulating streptavidin^{Bodipy} were treated with the translocator(s), and diffusion of the biotin markers through the pores was detected as an increase in streptavidin^{Bodipy} fluorescence as follows. Liposomes loaded with streptavidin^{Bodipy} (100 μM total lipids) were suspended in 50 mM sodium acetate buffer (pH 4.3) and 0.5 mM DTT containing 1 μM biocytin or 100 nM biotin-β-amylase. The net initial emission intensity (F_0) was determined after equilibration of the sample at 25 °C for 5 min. Translocators were added individually or together at a final concentration of 100 nM each, and samples were incubated at 20−23 °C for 15 min (protein:lipid ratio of 1:1000 for individual proteins and 1:500 when both proteins were added together). After re-equilibration at 25 °C, the final net emission intensity (F) of the sample was determined (i.e., after blank subtraction and dilution correction) and the enhancement of streptavidin^{Bodipy} fluorescence emission was estimated using F/F_0, which is proportional to the amount of biotinylated marker that can diffuse through membrane pores and bind to streptavidin^{Bodipy}. As a control, samples containing biotin-β-amylase were treated with Triton X-100 after F had been recorded to disrupt membranes and corroborate the binding activity between biotin-β-amylase and streptavidin^{Bodipy} (not shown).

Circular Dichroism (CD) Spectroscopy. Measurements were taken at 25 °C on a Jasco J-715 spectropolarimeter (Jasco Corp.) equipped with a Peltier effect device for temperature control. The scan speed was set to 20 nm/min with a 1 s response time, a 0.5 nm data pitch, and a 1 nm bandwidth. Far-UV spectra were recorded using 0.2 cm cells and protein concentrations of 2−3 μM in buffer E [10 mM sodium phosphate (pH 7.5)]. Six spectra were recorded and averaged for each sample.

Steady-State Fluorescence Spectroscopy. Steady-state fluorescence measurements were taken using a Fluorolog-3 photon-counting spectrofluorimeter equipped with a double monochromator in the excitation light path, a single emission monochromator, cooled photomultiplier tube housing, a 450 W xenon lamp, and a temperature-controlled sample holder.[20] For pore formation activity assays employing $Tb(DPA)_3^{3-}$ liposomes, excitation and emission wavelengths were set to 278 and 544 nm, respectively, and a 385 nm long pass filter was placed in the emission channel to block second-order harmonic light from passing through the emission monochromator. The

bandpass was typically 2 nm for excitation and 4 nm for emission. For experiments using streptavidin^{Bodipy}, samples were excited at 492 nm and the emission intensity was measured at 510 nm. Emission scans of intrinsic protein fluorescence were taken at 1 nm intervals between 285 and 405 nm, with an excitation wavelength of 278 nm. Emission scans for FRET experiments were conducted at 1 nm intervals between 490 and 560 nm, with an excitation wavelength of 485 nm.

Time-Resolved Fluorescence Spectroscopy. Time-resolved fluorescence measurements were taken in a Chronos multifrequency cross-correlation phase and modulation fluorometer equipped with a three-chamber cuvette holder for background subtraction from ISS (Champaign, IL). Samples were excited with a 470 nm laser diode (HBW 4 nm) filtered through a 472 nm interference filter (transmittance % HBW 10 nm) to eliminate spurious light. Emitted light was collected through a Melles Griot GG 495 sharp cutoff glass filter to eliminate scattered light and a Melles Griot 03SWP608 dielectric short-pass filter at 550 nm to minimize the contribution of direct excitation of Rh-PE. To avoid any polarization artifacts, measurements were taken under magic angle conditions using Glan-Thompson Prism Polarizers (10 mm × 10 mm aperture for excitation and 14 mm × 14 mm aperture for emission, set at 0° and 55° relative to the lab vertical axis, respectively). Fluorescence lifetimes were calculated by measuring the phase delay and modulation ratio spectra of samples in the 10−200 MHz frequency modulation range selecting 25 frequencies (25 °C). Blank subtraction was conducted using an equivalent sample without the fluorophore and using the algorithm described by Reinhart et al.[25] incorporated into the acquisition software. A solution of Fl (Invitrogen) in 0.1 M NaOH was used as a reference lifetime with a value of 4.05 ns,[21,26] and a total intensity similar to that of the measured sample (±10%).[27] One single-exponential lifetime of 4.05 ± 0.1 ns was obtained for this reference sample when measured against rhodamine B in methanol (lifetime of 2.5 ns[28]). The lifetime data were analyzed assuming different models, including monoexponential, multiexponential, or continuous lifetime distribution[29] decay models. The goodness of fit was determined by using the reduced χ^2 values. Uncertainties in the phase and modulation values were 0.2 and 0.004, respectively.

Membrane Binding FRET Measurements. The binding of PopB$^{S164C-Bodipy}$ or PopD$^{F223C-Bodipy}$ to membranes under equilibrium conditions was measured by FRET between a Bodipy-labeled translocator (donor or D) and Rh-PE as the acceptor (A), randomly distributed at the lipid bilayer. Four biochemically equivalent samples were prepared in parallel. Sample D_o (D only) contained 120 nM total translocator (an equimolar mixture of Bodipy-labeled translocator mutant and wild-type translocator was used to minimize Bodipy self-quenching) and POPC/POPS/cholesterol membranes (65:15:20 molar ratio) lacking Rh-PE. Sample DA (D plus A) contained the same protein mixture as in D_o and membranes containing Rh-PE (0.5% of the total lipids). Sample A_o (A only) contained 120 nM wild-type translocator and vesicles containing Rh-PE. The blank (B) sample contained 120 nM wild-type translocator and vesicles lacking Rh-PE. In all four samples, the total lipid concentration of the membranes was 0.3 mM. All samples were incubated at 25 °C for 30 min to permit complete insertion of translocator derivatives into the model membranes before spectral measurements were taken at 25 °C. FRET efficiency (E) was calculated as describe by Wu and Brand[30]

$$E = 1 - \frac{\langle \tau_{DA} \rangle_a}{\langle \tau_D \rangle_a}$$

where τ_{DA} and τ_D are the average amplitude-weighted lifetimes of D in the presence and absence of A, respectively. τ_{DA} and τ_D for DA and D_o samples were determined as described in Time-Resolved Fluorescence Spectroscopy using the A_o and B samples for blank subtraction, respectively. Phase delay and modulation ratio data best fit to two-exponential component models.

RESULTS

Purification of Homogeneous Chaperone−Translocator Complexes Containing Native PopB and PopD. Coexpression of hisPcrH with native PopD (or PopB) was achieved by using the pETDuet-1 system (Merk4Biosciences) as described in Experimental Procedures. The translocators were therefore purified in their native state, without modifications (i.e., no affinity tags or amino acid additions or deletions resulting from cloning into the expression vector). The absence of poly-His tags or fusion proteins (e.g., GST) is critical when electrostatic interactions and oligomerization of proteins are involved in the mechanism being investigated. Water-soluble hisPcrH−PopD and hisPcrH−PopB complexes were purified using IMAC and AEC. The IMAC step rendered a mixture of free hisPcrH together with hisPcrH−PopD (or hisPcrH−PopB) complexes (not shown). The AEC step separated the free hisPcrH chaperone and other minor contaminants from the hisPcrH−PopD (or hisPcrH−PopB) complex (Figure 1A,B). A major peak containing the hisPcrH−PopD complex eluted when the concentration of NaCl was 0.21 M. The free hisPcrH chaperone eluted later when the concentration of NaCl was 0.35 M (Figure 1A).

Size exclusion chromatography (SEC) analysis of the purified hisPcrH−PopD complex revealed a single symmetric peak (Figure S1 of the Supporting Information). When compared to the molecular mass standards, the hisPcrH−PopD complex eluted with an apparent molecular mass of 111 ± 1 kDa (expected value of 50.8 kDa), which suggested that the hisPcrH−PopD species may form 2:2 complexes. Similar SEC results have been described for *Shigella flexneri*[31] and *Aeromonas hydrophila*[32] translocators; however, analysis of these complexes has shown they adopt a 1:1 stoichiometry. Therefore, it seems that the purified hisPcrH−PopD complex forms an elongated 1:1 complex, as described for the *P. aeruginosa* CHA translocator and other related T3S proteins.[15,31,32]

In contrast to the hisPcrH−PopD complex, the hisPcrH−PopB complex eluted in two peaks during the AEC step (Figure 1B). The first peak eluted at 0.19 M NaCl, and a second peak eluted at 0.25 M NaCl. A third peak corresponding to the free hisPcrH chaperone eluted at a higher NaCl concentration (~0.30 M). SEC analysis of isolated fractions from the peaks revealed that the first peak corresponded mainly to a 1:1 hisPcrH−PopB complex (eluted at 13.9 mL), while the second peak contained a larger proportion of aggregates (Figure 1C). Interestingly, we noticed that the amount of the hisPcrH−PopB complex appearing as aggregates was affected by the concentration of the proteins (Figure S2B of the Supporting Information). The higher the protein concentration of the sample, the larger the amount of nonspecific hisPcrH−PopB

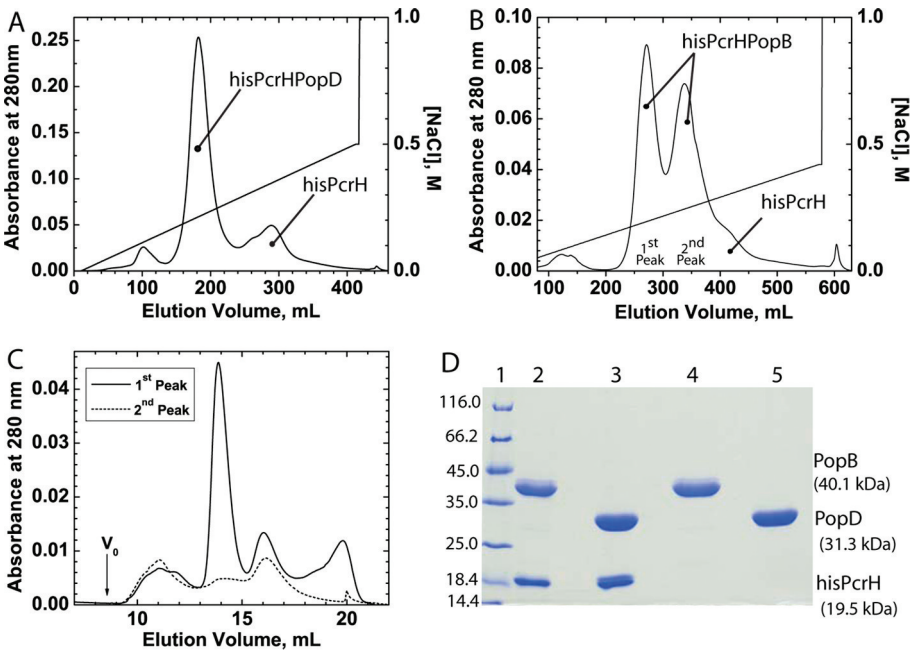

Figure 1. Purification of the hisPcrH–translocator complexes. (A) The fractions containing the hisPcrH–PopD complex isolated after the first IMAC purification step were dialyzed and loaded into a Q-Sepharose AEC column and eluted using a linear NaCl gradient. The peaks containing hisPcrH and the hisPcrH–PopD complex are indicated. (B) The hisPcrH–PopB complex was purified as described for the hisPcrH–PopD complex. The first two large peaks that eluted from the AEC column contained the hisPcrH–PopB complexes, and the shoulder that eluted around 400 mL contained hisPcrH. (C) SEC analysis of aliquots corresponding to the 1st peak and the 2nd peak illustrated in panel B. (D) SDS–PAGE analysis of purified proteins: lane 1, molecular mass markers; lane 2, hisPcrH–PopB complex; lane 3, hisPcrH–PopD complex; lanes 4 and 5, urea-isolated PopB and PopD, respectively.

aggregates observed, confirming the intrinsic tendency of the complex to aggregate in aqueous solution.[15,32]

The hisPcrH–PopB peak corresponding to the 1:1 complex was isolated and reanalyzed by SEC. A main symmetric peak eluted in the second SEC run (Figure S1 of the Supporting Information), indicating that the hisPcrH–PopB complex was stable in solution and ran with a hydrodynamic radius equivalent to that of a 95 ± 3 kDa globular protein. Because the expected molecular mass of a 1:1 complex is 59.6 kDa, this result suggested that the hisPcrH–PopB complex adopted an elongated conformation rather than a globular shape, as shown previously for the homologue protein AopB.[32]

We have therefore optimized the procedures to obtain both hisPcrH–PopD and hisPcrH–PopB complexes purified to apparent homogeneity (Figure 1D, lanes 2 and 3, and Figure S1 of the Supporting Information).

Spectroscopic and Functional Characterization of the Purified Chaperone-Associated Proteins. The far-UV CD spectrum of the purified chaperone hisPcrH revealed a typical all-α protein, with double minima around 222 and 209 nm (Figure 2A). These data correlated well with the recently determined three-dimensional structure of the $PcrH_{21-160}$ fragment, which consists of α-helical tetratricopeptide repeats.[33,34] The far-UV CD spectrum of the hisPcrH–PopD complex suggested that PopD also contains a high α-helical structure content (Figure 2A and ref 33). The band with a minimum at 208 nm had a larger intensity than that at 222 nm, suggesting the presence of other secondary structural elements in this complex.[35] The far-UV CD spectrum of the hisPcrH–PopB complex was similar to that of the hisPcrH–PopD complex, but the intensity of the bands was lower, suggesting

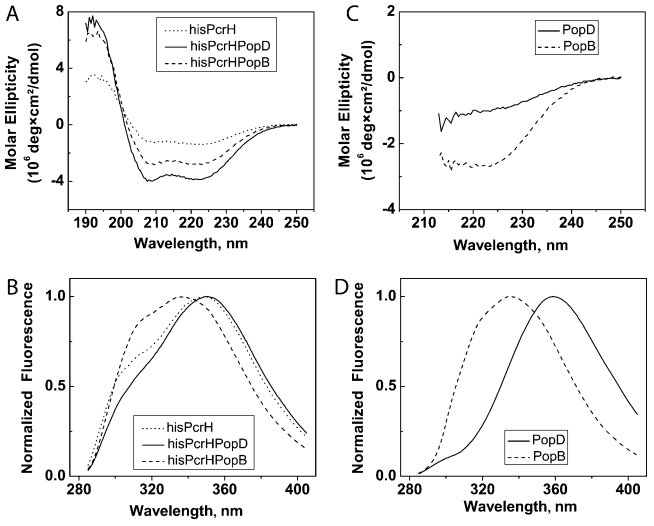

Figure 2. Characterization of purified translocators. (A) Far-UV CD spectra of the SEC-isolated hisPcrH, hisPcrH–PopD complex, and hisPcrH–PopB complex recorded in buffer E, at a total protein concentration of 3.0 μM. (B) Normalized fluorescence emission spectra of hisPcrH, the hisPcrH–PopD complex, and the hisPcrH–PopB complex recorded in buffer E. The excitation wavelength was 278 nm, and the total protein concentration was 2.4 μM. (C) Far-UV CD spectra of purified PopD and PopB recorded in 20 mM phosphate buffer (pH 7.5) supplemented with 6 M urea, with a protein concentration of 2.4 μM. (D) Normalized fluorescence emission spectra of PopD and PopB in 20 mM phosphate buffer (pH 7.5) supplemented with 6 M urea. The excitation wavelength was 278 nm, and the total protein concentration was 2.4 μM.

dx.doi.org/10.1021/bi200905x | *Biochemistry* 2011, 50, 7117–7131

that PopB is less α-helical than PopD when bound to the PcrH chaperone.

Additionally, we evaluated the local environment around the aromatic residues of the *P. aeruginosa* PAO1 purified proteins. The hisPcrH chaperone contains one Trp and nine Tyr residues, while PopD contains two Tyr and two Trp residues; PopB contains one Tyr and one Trp. The emission fluorescence spectra of hisPcrH showed a peak with a maximum at 349 nm (Figure 2B), indicating that the Trp residue was located in a polar environment, in agreement with the position observed in the structure determined via X-rays.[34] The shoulder around 303 nm corresponded to the emission of multiple Tyr residues. The hisPcrH–PopD complex presented an emission fluorescence spectrum similar to that of hisPcrH, with a maximum at 351 nm. This red-shifted maximum suggested that both the central and C-terminal Trp residues of PopD reside in a polar environment. In contrast, the emission fluorescence spectrum of the hisPcrH–PopB complex showed a maximum at 337 nm, suggesting that the Trp residue of PopB was located in a nonpolar environment (Figure 2B).

The pore formation activity for both purified proteins was analyzed using the fluorescence assay previously described by us.[22] In this assay, a fluorescent marker was encapsulated into liposomes and a quencher was added to the external buffer solution. A high-fluorescence intensity signal indicated that the membrane was intact and the quencher could not contact the fluorophore. If a transmembrane pore is formed upon addition of protein, the fluorophore becomes accessible to the quencher and the magnitude of the fluorescent signal decreases. Both PopB and PopD dissociate from PcrH in vitro when the solution pH decreases to 5.3, forming heterogeneous protein aggregates.[15] These dissociated protein aggregates form pores in model membrane systems;[16] however, the translocators are presumably secreted as monomers in vivo and in the proximity of the target membrane. Under these circumstances, binding to the membrane can precede any protein–protein association. We therefore reasoned that the dissociation of the translocators from the chaperone in the presence of liposomes would more accurately represent in vivo conditions.

When separated from PcrH when the pH decreased from 8.0 to 5.1 in the presence of lipid membranes, PopB, PopD, and the equimolar mixture of these proteins were able to form pores (Figure S3A of the Supporting Information). Interestingly, in contrast with the results observed when protein aggregates were used, no synergy was observed between PopB and PopD.[16] It is therefore clear that the history (i.e., aggregation) of the proteins may affect the mechanism by which the translocators form a pore. Because the sequence of the events that leads to the assembly of a membrane-inserted translocon is far from understood, an experimental procedure that replicates the in vivo scenario encountered by the proteins after being secreted through the T3S needle is desirable.

An Efficient Procedure for Isolating PopB and PopD Derivatives. Insights into the mechanism of insertion of protein into lipid bilayers and the interaction of proteins with membranes can be obtained by fluorescence spectroscopy and site-directed fluorescence labeling.[36] A Cys residue is introduced by site-directed mutagenesis at a single site in the protein, and the unique Cys is specifically labeled with the fluorophore of choice. Protein–membrane association and protein–protein interactions can therefore be studied using FRET, excitation energy migration (homo-FRET), or fluorescence quenching.[37−39]

P. aeruginosa PAO1 translocators do not contain Cys residues, and therefore, they are optimal substrates for site-directed fluorescence labeling. However, the labeling of isolated translocators in solution is hampered by their intrinsic tendency to aggregate. Introduced Cys residues can be alternatively labeled while the translocator is still bound to the chaperone PcrH. We noticed that in the recently determined X-ray structure of PcrH the three Cys residues are not exposed to the solvent,[34] and therefore, we reasoned that the specific labeling of the translocators may be possible even in the presence of the chaperone. However, our initial labeling reactions demonstrated that the chaperone was also efficiently labeled with thiol-specific probes (not shown).

Analysis of the solvent exposure for the native hisPcrH Cys revealed that on average, 2.20 ± 0.03 Cys residues reacted with Ellman's reagent (DTNB). Interestingly, incubation of hisPcrH with 6 M guanidinium chloride at 37 °C for 1 h did not increase the reactivity of the hisPcrH Cys residues to DTNB, suggesting that a portion of those residues were forming intra- or intermolecular disulfide bonds. SEC analysis of purified hisPcrH samples revealed a first small peak eluted at 14.3 mL and a large second peak eluted at 15.3 mL (Figure S4A of the Supporting Information). Nonreducing SDS–PAGE analysis of the two peaks revealed that hisPcrH formed intermolecular disulfide bonds in solution (Figure S4B of the Supporting Information). Hence, it is clear from these data that the structure of PcrH in solution is dynamic, and the side chains of the amino acids surrounding the Cys residues move and expose the sulfhydryl groups to the solvent (see below).

Any attempts to replace all three Cys residues in PcrH with nonreactive residues (Ala or Ser) rendered a chaperone that can no longer bind PopD (not shown). Therefore, the interpretation of the fluorescence signal and observed spectral changes derived from the single fluorescently labeled translocators would be veiled by the presence of a labeled chaperone. The spectroscopic characterization of the translocon assembly mechanism, therefore, requires an efficient separation of the labeled translocators from the labeled hisPcrH chaperone prior to the analysis.

We took advantage of the poly-His tag located at the N-terminus of the chaperone to isolate labeled translocators. After being labeled, the translocators were separated from hisPcrH by binding of the hisPcrH–PopD (or hisPcrH–PopB) complex to an IMAC column and a subsequent elution of PopD (or PopB) with buffer containing 6 M urea. Urea did dissociate PopD or PopB from their cognate chaperone without affecting the interaction of hisPcrH with the IMAC column (Figure 1D, lanes 4 and 5). Therefore, the single-Cys translocator mutants can be labeled while still bound to hisPcrH and separated from the chaperone in a subsequent step. This is a simple and efficient procedure for obtaining the translocator derivatives required for the structural and functional characterization of the T3S translocon (e.g., single fluorescently labeled translocators).

Spectroscopic and Functional Characterization of Urea-Isolated PopB and PopD. We analyzed the structural and functional properties of the urea-isolated translocators using mass spectrometry, far-UV CD, intrinsic protein fluorescence, and pore formation assays using model membranes. The molecular mass of urea-isolated PopB and PopD was

determined using ESI-ion trap mass spectrometry as detailed in Experimental Procedures. Only one species was detected for each protein sample with a molecular mass of 40058 Da for PopB (expected value of 40061 Da) and 31308 Da for PopD (expected value of 31309 Da).

The polarity around the Trp residues for the urea-isolated PopD and PopB was similar to the polarity observed for the proteins complexed with the hisPcrH chaperone (Figure 2D). PopD and PopB in urea presented fluorescence emission maxima at 358 and 334 nm, respectively. The far-UV CD negative band at 222 nm observed for PopB in 6 M urea suggested that PopB conserved a high proportion of its α-helical structure even in the presence of the chaotropic agent (Figure 2C). However, the far-UV CD spectrum of PopD in 6 M urea revealed that a sizable portion of the secondary structure of this translocator was lost in the presence of the chaotropic agent.

Despite the differences observed in their secondary structure, both urea-isolated PopB and PopD conserved their pore forming abilities at a mildly acidic pH (Figure S3B of the Supporting Information). The pore formation activity profiles of urea-isolated translocators were very similar to those observed when the translocators were directly dissociated from the chaperone by reducing the pH of the medium (Figure S3 of the Supporting Information). Altogether, our data indicated that the purification procedure described above constitutes a simple and efficient alternative for obtaining highly pure and active PopD, PopB, and their mutant derivatives.

Optimization of a Model System for Analyzing the Membrane-Inserted State of the Translocators. Unambiguous interpretation of structural data requires that the components under investigation adopt a uniform conformational state. For the structural analysis of assembled T3S translocons, it is essential that the measured fluorescent signal come from probes located in the same conformation (i.e., membrane-inserted translocons). We therefore optimized our model system to maximize the assembly and insertion of the T3S translocators. Three factors affect the assembly of active transmembrane pores in our experimental system: (i) the pH of the medium, (ii) the presence of negatively charged phospholipids, and (iii) the concentration of cholesterol in the target membrane.

In membranes containing a mixture of the lipids commonly present in mammalian plasma membranes (i.e., POPC, POPE, POPS, and sphingomyelin) and 15 mol % cholesterol, the maximal activity for PopB (~60%) was observed at pH $\leq$5.1 (Figure 3A). For PopD, the maximal activity (~90%) was observed at pH <5. Interestingly, the activity of PopD was lower than the activity of PopB at pH >5.1, but it surpassed that observed for PopB at pH <4.8, suggesting that the insertion of PopD into membranes is more dependent on acidic residue protonation than the insertion of PopB.

When a constant POPC:POPE:POPS:sphingomyelin molar ratio was maintained in the absence or presence of a high level of cholesterol (45 mol %), the pore forming activity of the translocators was less effective than that observed with 15 mol % cholesterol (not shown). Because the activities of PopD and PopB plateau below pH 4.5 at intermediate cholesterol concentrations, we selected pH 4.0–4.3 and 20 mol % cholesterol for our assays to maximize the formation of uniform membrane-inserted translocons.

Negatively charged phospholipids affect the degree of insertion of T3S translocators.[15,16] We therefore analyzed the effect of POPS on the activity of urea-isolated PopB and PopD in

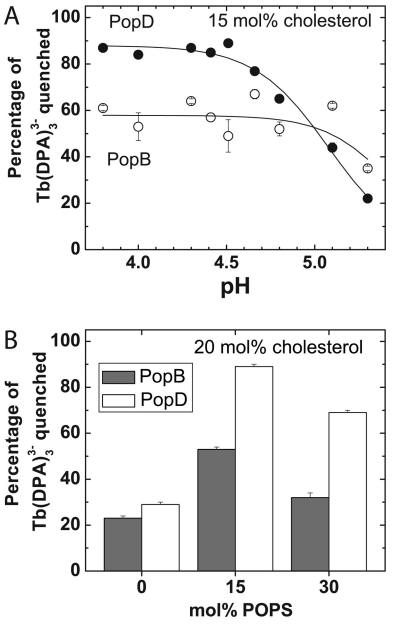

Figure 3. Effect of pH and lipid composition on the pore forming activity of the urea-isolated translocators. Pore formation was determined as the percentage of the encapsulated $Tb(DPA)_3^{3-}$ that was quenched by EDTA as detailed in Experimental Procedures. (A) Urea-isolated PopB or PopD was directly diluted into a solution of 50 mM sodium acetate buffered at the indicated pH, containing membranes. The pore forming activity of the urea-isolated translocators increased at acidic pH. The total lipid concentration was 0.1 mM, and the liposomes consisted of 35 mol % POPC, 15 mol % POPS, 20 mol % POPE, 15 mol % SM, and 15 mol % cholesterol. The protein:lipid ratio was 1:1000. (B) Effect of POPS on the pore formation activity of urea-isolated translocators. The activity was measured as described for panel A; the pH was buffered at 4.3, and the lipid mixture consisted of POPC, 20 mol % cholesterol, and the indicated concentration of POPS.

membranes containing POPC and a fixed amount of cholesterol (20 mol %). Addition of 15 mol % POPS increased 2-fold the activity of PopB and >3-fold the activity of PopD (Figure 3B). Doubling the amount of POPS to 30 mol % was not as effective as the addition of only 15 mol % POPS. Thus, to maximize the conformational homogeneity of membrane-inserted translocators and to minimize any effect caused by the variability of the lipid composition of the system, we chose the simplest membrane model system that maximized the formation of transmembrane pores, a 65:15:20 POPC:POPS:cholesterol molar ratio.

The pore forming activity of urea-isolated PopD, PopB, and a 1:1 mixture of the translocators was studied using this model system. Maximal activity for PopB and PopD was observed below pH 4.8 and 4.3, respectively (Figure 4A). Interestingly, no additive or synergic effect was detected at higher pH, where the individual proteins exhibited intermediate pore forming activity. Maximal pore formation using these experimental conditions was observed when the protein:lipid ratio was ~1:3000 (Figure 4B).

High Translocator:Lipid Ratios Produced Liposome Aggregation. Our initial attempts to visualize the membrane-inserted PopD using transmission electron microscopy and 2% uranyl acetate as a contrast agent revealed that even when used at a 1:1000 protein:lipid ratio, PopD disrupted the liposomes forming tubular membrane structures (not shown).

dx.doi.org/10.1021/bi200905x | Biochemistry 2011, 50, 7117–7131

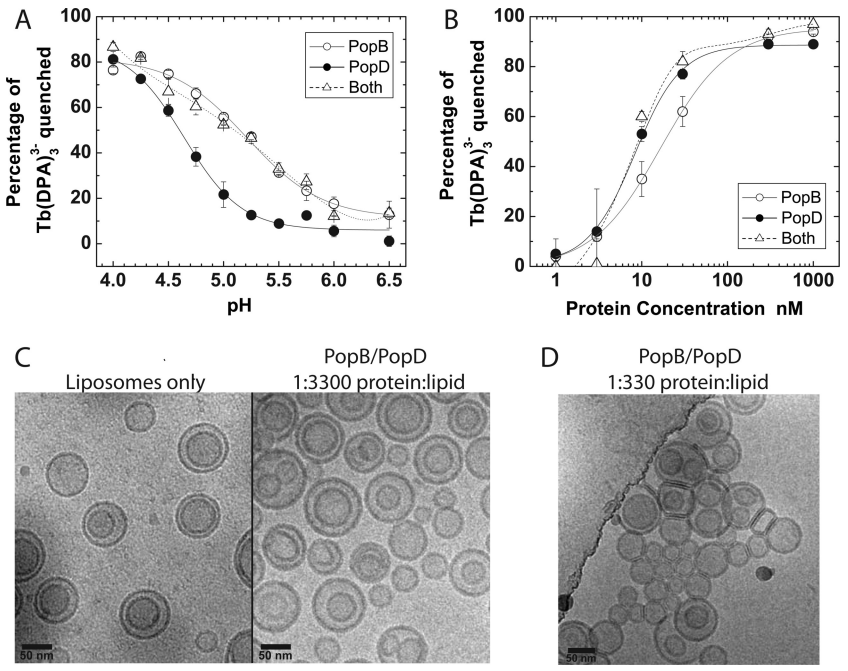

Figure 4. Pore forming activity of the urea-isolated translocators. Pore formation was determined as the percentage of the encapsulated $Tb(DPA)_3^{3-}$ that was quenched by EDTA as detailed in Experimental Procedures. (A) Urea-isolated PopB, PopD, or an equimolar mixture of both proteins was diluted into a buffer solution containing membranes at the indicated pH. The total concentration of lipids was 0.15 mM. The total protein concentration was 60 nM for the PopB and PopD traces (protein:lipid ratio of 1:2500) and 120 nM when PopB and PopD were added together (protein:lipid ratio of 1:1250). (B) Concentration-dependent pore formation by PopD, PopB (protein:lipid ratio ranged from $1:10^5$ to 1:100), or an equimolar mixture of both proteins diluted into buffer D containing 0.1 mM total lipids. When both proteins were added together, the sample contained twice as much total protein vs the concentration indicated in the graph (protein:lipid ratio ranged from $1:5 \times 10^4$ to 1:50). (C) Cryo-electron micrographs of liposomes with and without PopB and PopD at the indicated protein:lipid ratios. Buffer B was added to the control sample with only liposomes to assess any effect of the residual urea concentration on membrane structure. The lipid concentration was 5 mM in all cases, and the total protein concentration was 1.5 or 15 μM. The POPC:cholesterol:POPS molar ratio was 65:20:15 in all panels.

We therefore analyzed the aggregated state of the liposomes using DLS. Isolated liposomes, incubated at pH 4.0, showed a single-particle size distribution with an average of 78 nm [expected value of ~100 nm (see Figure S7 of the Supporting Information)]. However, the incubation of the same liposomes with PopD, PopB, or an equimolar mixture of both translocators, using a 1:1000 protein:lipid molar ratio, shifted the average size distribution to 264, 342, or 164 nm, respectively. These data suggested that at this protein:lipid ratio the translocators caused aggregation of the vesicles, especially when added individually. Little or no aggregation was observed when lower protein:lipid ratios were used (Figure S7 of the Supporting Information). Therefore, when structural studies are performed in model systems, it is important to confirm that the size of the vesicles is not altered by the addition of the proteins. If aggregation occurs, the structure adopted by the proteins when bound to membranes may differ from the structure adopted upon formation of discrete transmembrane pores.

We used cryo-EM to directly visualize the liposomes before and after incubation with the translocators and to determine the optimal protein:lipid ratio to be used in our studies. Surprisingly, extruded liposomes prepared with a 65:15:20 POPC:POPS:cholesterol molar ratio were mostly multilamellar (Figure 4C). Using different protein:lipid ratios, we found that addition of an equimolar mixture of both proteins at a protein:lipid ratio at or below 1:3300 did not alter the liposomal structure (Figure 4C and Figure S7 of the Supporting Information). Higher protein concentrations (e.g., 1:330) caused liposome aggregation (Figure 4D and Figure S7 of the Supporting Information), but no tubular structures were observed by cryo-EM.

PopB and PopD Form Discrete and Stable Membrane Pores. We analyzed the ability of the urea-isolated translocators to form discrete and stable pores in liposomes encapsulating the streptavidin^{Bodipy} fluorescent marker (~5 nm diameter). In contrast to those of fluorescein (Fl) and Fl derivatives (e.g., calcein and Oregon green), the fluorescent properties of the Bodipy dye are stable at acidic pH.[40] Binding of biocytin (biotin moiety covalently attached to the amino acid Lys, ~1 nm in diameter) or biotin attached to the protein β-amylase (~4 nm in diameter) or to streptavidin^{Bodipy} (~5 nm in diameter for the monomer) produces a 2- or 3-fold enhancement, respectively, in the fluorescence intensity of the streptavidin^{Bodipy} marker (not shown and refs 41 and 42). When the biotin-labeled molecules were externally added to the sample containing intact liposomes, no fluorescence change was detected on the encapsulated streptavidin^{Bodipy}. Neither biocytin nor proteins like β-amylase or streptavidin^{Bodipy} can pass through the membrane unless a pore is formed. The size of the pore will dictate which molecules can cross the membrane. Addition of the translocators produced a fluorescence intensity increase only for the samples containing biocytin, and not for the ones containing biotin-β-amylase. These results indicated that the transmembrane pores formed by PopB and PopD were >1 nm in diameter, but not large enough to allow the passage of the β-amylase protein or the encapsulated streptavidin^{Bodipy} (Figure 5A).

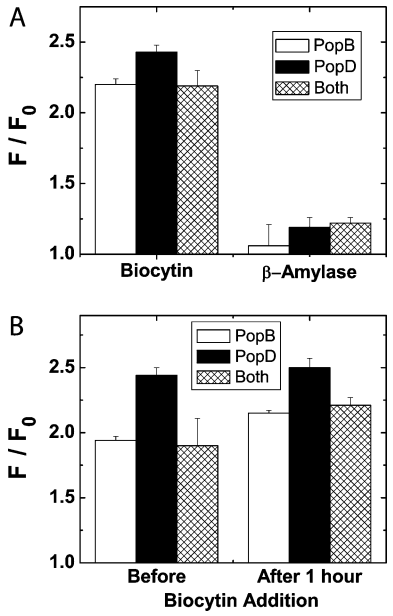

Figure 5. PopD and PopB form discrete and stable pores in model membranes. (A) The passage of biocytin (~10 Å diameter), biotin-labeled β-amylase (~50 Å diameter), or streptavidin^{Bodipy} (~50 Å diameter) through the pores formed by PopD, PopB, or an equimolar mixture of the translocators was measured as detailed in Experimental Procedures. The total lipid concentration was 100 μM, and the protein concentration of the proteins was 100 nM (protein:lipid ratio of 1:1000 for individual proteins and 1:500 when added together). The fluorescence intensity of encapsulated streptavidin^{Bodipy} was measured before (F_0) or after the incubation for 60 min at 25 °C with the translocators (F). Only biocytin was able to diffuse through the formed pores. (B) The stability of the formed pores was examined by measuring the increase in the fluorescence intensity of encapsulated streptavidin^{Bodipy} when biocytin was present in the external buffer solution before the addition of the translocators, or added after incubation for 1 h with the translocators. The discrete pores formed by PopB, PopD, and an equimolar mixture of the proteins remained open after incubation for 1 h.

The stability of the formed pores was determined by adding the enhancer (biocytin) before or after the addition of the translocators. If the pores are stable, the enhancement of the fluorescence intensity of streptavidin^{Bodipy} will be observed when biocytin is added before or after the incubation with the translocators. In contrast, if the formed pores are not stable and close, the fluorescence will increase only when biocytin is present before the addition of the translocators, and not when added after the incubation. Because the fluorescence intensity increased in both cases (Figure 5B), it is clear that the formed pores remained stably open for at least 1 h in this model system. Control experiments without translocators did not show significant fluorescence change.

PopB and PopD Binding to Membranes Also Required Acidic pH. To precisely assess the binding of the translocators to the target membrane, we introduced single Cys residues into PopB at a location close to a predicted TM segment (S164), and in PopD at a location that was found to be exposed to the aqueous solvent in the membrane-bound complex [F223 (M. Buckner, unpublished results)]. The Cys residues were labeled with Bodipy. As mentioned above, the emission properties of Bodipy are not sensitive to the polarity of the environment and are not affected by pH in the range used in this work.[40] Bodipy-labeled translocators were isolated from the hisPcrH chaperone by elution with 6 M urea as described for the wild-type proteins (Figure 1). The pore forming activity of the Bodipy-labeled translocators was similar to the activity of the wild-type proteins.

We first analyzed the binding of the translocators by using FRET. FRET is an effective method for identifying protein–membrane binding under equilibrium conditions (e.g., refs 37 and 43–46). A typical FRET membrane binding experiment requires two fluorescent dyes, a donor (D) located at a specific site in the protein and an acceptor (A) distributed on the surface of the membrane. The Bodipy dye covalently attached to PopB^{S164C} (or PopD^{F223C}) was used as the D dye in our FRET experiments, while Rh-PE incorporated into the membrane was the A dye. After excitation by the absorption of a photon, Bodipy can transfer its excited-state energy to Rh-PE. The efficiency of this transfer depends on, among other things, the extent of overlap of the D emission and the A absorption spectra, the relative orientation of the transition dipoles of D and A, and, more importantly, the distance between the D and A dyes. The distance at which the efficiency of FRET from D to A is 50% is designated R_0 (the R_0 is ~52 Å for the Bodipy/Rh-PE pair[44]). Because the FRET efficiency is strongly dependent upon the actual distance separating D and A, FRET will be detected if the dyes are within 95 Å of each other, and it will be maximal when the dyes are separated by less than 24 Å. While considerable FRET efficiency is expected for Bodipy dyes close to the membrane surface (i.e., membrane-bound translocators), no significant FRET is expected for unbound proteins because they will reside more than 100 Å from the membrane surface. FRET efficiency was estimated using the amplitude-weighted average lifetime of D in the presence ($\langle\tau_{DA}\rangle_a$) or absence ($\langle\tau_D\rangle_a$) of A. The use of lifetime determinations over steady-state measurements is advantageous because it minimizes the problems associated with the quantification of D in the presence and absence of A.[30] Two exponential components were used to fit the lifetime data (Figure S8 and Table S1 of the Supporting Information). The use of additional exponential components or lifetime distributions in the analysis did not improve the fit of the data. Binding of the translocators was strongly dependent on the pH of the medium (F. B. Romano et al., manuscript in preparation). We report here the FRET efficiency at binding saturation (pH 4) and at a point of weak binding (pH 6). The PopB FRET efficiency was 40% lower at pH 6.0 than at pH 4.0, while the PopD FRET efficiency was more than 80% lower at pH 6.0 than at pH 4.0 (Figure 6).

The pH-dependent binding of the translocators was independently assessed by separation of the bound and unbound protein fractions using a sucrose step gradient and ultracentrifugation as described in Experimental Procedures.[15,23,47] Given the different densities of proteoliposomes and unbound proteins, proteoliposomes containing the bound protein float to the top of the sucrose cushion while unbound protein remains at the bottom.[23] Bodipy-labeled translocators were individually incubated with membranes at the pH of maximal pore formation activity [pH 4.0 (see Figure 4)] and at pH 6.0, where the pore forming activity for PopB was significantly lower, and almost null for PopD. The amount of protein isolated in the top fraction (i.e., membrane-bound translocator) was quantified using SDS–PAGE followed by fluorescence scanning with a phosphorimager and reported as the fraction of

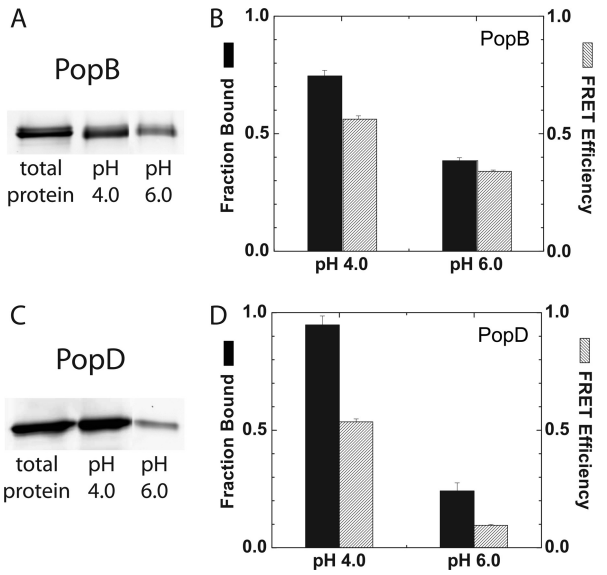

Figure 6. Acidic pH enhances translocator–membrane binding. (A) $PopB^{S164C-Bodipy}$ membrane binding was measured using the liposome flotation assay described in Experimental Procedures. $PopB^{S164C-Bodipy}$ (0.4 μM) was incubated with membranes (2 mM total lipids) for 1 h at 20–23 °C. Typical SDS–PAGE analysis was conducted showing the amount of total protein added, and the amount of bound protein isolated after incubation with membranes at the indicated pH. The protein:lipid ratio was 1:5000. Gels were scanned for Bodipy fluorescence using a phosphoimager. (B) Quantification of $PopB^{S164C-Bodipy}$ binding measured by the liposome flotation assay (fraction bound, black bars). Data were normalized against the total amount of protein used in the binding reaction. Each bar represents the average and range of at least two independent experiments. FRET efficiency (gray bars) for $PopB^{S164C-Bodipy}$ binding determined by time-resolved FRET as described in Experimental Procedures. $PopB^{S164C-Bodipy}$ (120 nM) was incubated with membranes (total lipid concentration of 0.3 mM) as described for panel A (protein:lipid ratio of 1:2500). Each bar represents the average and range of two independent experiments. (C and D) Analysis of $PopD^{F223C-Bodipy}$ binding as described for panels A and B, respectively, for $PopB^{S164C-Bodipy}$. The POPC:cholesterol:POPS molar ratio was 65:20:15 in all panels.

the total protein bound to membranes (Figure 6). At pH 4.0, more than 70% of the added $PopB^{S164C-Bodipy}$ and more than 90% of the added $PopD^{F223C-Bodipy}$ were isolated in the fraction containing the membranes. In contrast, the level of membrane binding at pH 6.0 was only 40 and 25% for PopB and PopD, respectively. These data were consistent with the amount of protein binding observed by FRET. Therefore, we concluded from these complementary and independent approaches that the binding of PopB and PopD to the membrane was stronger at the pH of maximal activity and decreased when the pH was closer to neutral.

PopB Interacts with PopD on Model Membranes. We have shown that PopD and PopB have different optimal pH and lipid composition requirements to form pores in membranes (Figures 3 and 4). Surprisingly, the pore forming properties of the translocators when added together were similar to those observed for PopB alone. No synergic effect between PopB and PopD was observed under our experimental conditions (see Discussion). Do the translocators interact with each other at all? We took advantage of the fluorescence properties of Bodipy to assess PopB–PopD association on membranes.

The fluorescence properties of Bodipy dyes change significantly when they are brought into the proximity of one another. At distances of orbital–orbital contact, the emission intensity and lifetime of the sample decrease significantly, presumably because of the formation of nonfluorescent Bodipy dimers.[48] The proximity of Bodipy dyes at longer distances (i.e., between ~20 and 85 Å) is detected by the decrease in the anisotropy of the sample (depolarization) caused by energy migration.[48,49] Protein–protein association can be determined in principle by changes in the fluorescence properties of the sample mentioned above when Bodipy-labeled proteins are employed.[50] We used a Bodipy-labeled PFO derivative (see the Supporting Information) as a control for how protein–protein association on membranes affects the fluorescence properties of Bodipy. PFO is well-characterized cholesterol-dependent cytolysin that forms oligomeric complexes on lipid membranes.[51] These complexes are formed by association of up to 50 monomers in a circular ringlike oligomer on the membrane surface. The rings are ~300 Å in diameter.[52,53] We compared a membrane-assembled sample containing 100% labeled PFO, where the effects on the fluorescence properties will be maximal, with a sample containing only 10 mol % labeled protein (i.e., only 5 of 50 monomers will be labeled on average in each oligomeric complex). The diluted sample exhibited a 4.5-fold increase in emission intensity and a >2-fold increase in the amplitude-averaged fluorescence lifetime (Table 1), showing that addition of unlabeled PFO separated the PFO^{Bodipy} molecules, increasing the distance between probes.[48] The increase in the distance between probes, caused by the intercalation of unlabeled proteins, also weakened the depolarization of the sample emission caused by Bodipy–Bodipy energy migration [i.e., the anisotropy increased (Table 1 and ref 54)].

We assessed the interaction between PopB and PopD using $PopD^{Bodipy}$ and analyzed the changes in the fluorescence properties of the sample when the labeled translocator was mixed with unlabeled PopB (and vice versa). As expected for the formation of mixed protein complexes containing both PopB and PopD in the membrane, dilution of $PopD^{Bodipy}$ with unlabeled PopB increased the emission intensity and the amplitude-averaged fluorescence lifetime of Bodipy (Table 1). Upon comparison to the data obtained for the PFO oligomer, it is clear that unlabeled PopB intercalated between labeled PopD proteins when bound to the membrane. The significant but relatively smaller increase in the anisotropy for Bodipy-labeled translocators suggested that PopD and PopB formed heteromeric complexes smaller in size than the large ~300 Å diameter rings formed by PFO, as Bodipy–Bodipy energy migration occurs only at distances of <100 Å. Similar changes were detected when $PopB^{Bodipy}$ was diluted with unlabeled PopD. The smaller changes in the fluorescence parameters observed for $PopB^{Bodipy}$ reflected the lower percentage of labeling of this derivative (68% vs 96% for $PopD^{Bodipy}$). Thus, we conclude that when added together, PopB associated with PopD to assemble pore-forming complexes on model membranes.

DISCUSSION

Structural and functional characterization of the T3S translocators is inherently difficult given the nonpolar nature of the proteins and their tendency to aggregate in solution. Coexpression of T3S recombinant translocators in the presence

Table 1. Bodipy Detected Protein−Protein Interaction in Intact Membranes[a]

fraction of protein added					
PFO^{Bodipy}	PFO	I (relative units)	I_{10}/I_{100} (relative units)	r	$\langle\tau\rangle_\alpha$[b] (ns)
1	–	1.84 ± 0.09		0.050 ± 0.005	1.55 ± 0.01
1	9	8.27 ± 0.07	4.5 ± 0.2	0.123 ± 0.005	4.75 ± 0.01
$PopD^{Bodipy}$	PopB				
1	–	6.5 ± 0.2		0.161 ± 0.004	2.56 ± 0.03
1	9	14.4 ± 0.2	2.22 ± 0.08	0.186 ± 0.009	3.90 ± 0.03
$PopB^{Bodipy}$	PopD				
1	–	4.32 ± 0.04		0.185 ± 0.003	3.24 ± 0.02
1	9	7.1 ± 0.2	1.63 ± 0.02	0.226 ± 0.003	4.93 ± 0.04

[a]Relative fractions of proteins added are indicated. Labeled and unlabeled proteins were mixed in buffer B supplemented with 6 M urea and 20 mM Gly solution prior to dilution in buffer D in the presence of membranes. The final fluorescence parameters measured for the different samples are indicated: I, fluorescence emission intensity; I_{10}/I_{100}, ratio of the fluorescence emissions of diluted to undiluted labeled protein samples; $\langle\tau\rangle_\alpha$, amplitude-weighted average fluorescence lifetime. The fluorescence lifetime of Bodipy in 50 mM sodium acetate (pH 4.0) was 5.85 ns. The fluorescence lifetime of monomeric PFO^{Bodipy} in buffer C was 5.51 ns. Labeling efficiencies were 100, 96, and 68% for PFO^{Bodipy}, $PopD^{F223C-Bodipy}$, and $PopB^{S164C-Bodipy}$, respectively. The average and range of at least two determinations are shown. Protein:lipid ratios were 1:2500 for fluorescence lifetimes and 1:10000 for steady-state determinations. [b]Time-resolved fluorescence data for 10% labeled PFO best fit to a single-exponential component. The remaining data best fit to a two-exponential component (see Table S1 of the Supporting Information).

of their cognate chaperone renders soluble protein complexes and allows their purification in large quantities.[15,31−33] However, the analysis of individual T3S translocators requires their separation from the chaperone prior to their assembly into membranes. These separations have been achieved by reducing the pH of the medium[15,31] or by the inclusion of mild detergents.[31] Unfortunately, upon dissociation from the PcrH chaperone, both PopB and PopD form large and nonuniform protein aggregates[15] that make it difficult to characterize the protein−membrane and protein−protein association processes. Furthermore, we observed that during the acidification of the medium to separate the translocators from the chaperone, PcrH precipitates, carrying considerable amounts of the purified translocators (Figure S5 of the Supporting Information). Thus, the precise characterization of the assembly of the T3S translocon into membranes required a more efficient experimental approach for isolation of active translocators.

We have found in these studies that PopB (as well as PopD) can be purified as a homogeneous complex with the cognate chaperone hisPcrH and be effectively dissociated and isolated from hisPcrH using urea. In contrast to PopD, which lost most of its secondary structure, PopB retained a high proportion of its secondary structure after solubilization in 6 M urea. The blue-shifted intrinsic fluorescence spectra of urea-solubilized PopB suggested that the Trp located at the N-terminus of a predicted TM segment (residues 169−187) remained located in a nonpolar environment even in its denatured state. As expected for proteins that are proposed to travel in an unfolded state through the T3S needle and to be released in the proximity of the target membrane, both urea-isolated translocators formed discrete and stable TM pores upon dilution in the presence of lipid bilayers. The pore forming properties of urea-isolated PopB and PopD were consistent with those described previously for translocators isolated using low pH.[16] Interestingly, quantitative assessment of binding of PopB and PopD to membranes showed that acidic pH was required not only for membrane insertion but also for a stable protein−membrane interaction. In summary, we have established an efficient experimental procedure for isolating native and modified forms of PopB and PopD and for specifically labeling the translocators with fluorescent or other types of probes (e.g., cross-linkers). Isolated translocators were assembled on model membranes where they form discrete and stable pores. Moreover, our spectroscopic examination of Bodipy-labeled translocators showed that when added together, PopB intercalates with PopD on membrane-assembled complexes.

Purification of isolated recombinant translocators has proven to be a difficult task. PopD cloned in pET-based vector systems produced large amounts of protein, but mostly as inclusion bodies. The yield of water-soluble PopD can be improved by expression at a low temperature (i.e., ∼18 °C), but water-soluble PopD forms aggregates (ref 15 and data not shown). PopB is toxic for *Escherichia coli* cells and cannot be stably produced (data not shown). Schoehn et al.[15] elegantly solved these problems by coexpressing the translocators with their cognate chaperone, PcrH. The water-soluble 1:1 PcrH−PopD complex was obtained in large amounts, and the structural characterization of PopD showed it adopts a molten globular conformation.[33] Less is known about the structure of PopB, given that only minor amounts of a homogeneous PcrH−PopB complex were obtained using this procedure.[15,32]

We found that the purified hisPcrH−PopB complex can remain soluble and nonaggregated in aqueous solutions at relatively low concentrations (Figure 1 and Figure S1 of the Supporting Information). The structure of the purified hisPcrH−PopB complex was analyzed using a combination of CD and fluorescence spectroscopy (Figure 2). Far-UV CD analysis revealed that PopB had less α-helical content than PopD when bound to hisPcrH. However, in contrast to the low secondary structure content observed in urea-isolated PopD, urea-isolated PopB retained a considerable amount of secondary structure. Furthermore, the only Trp of PopB was located in a nonpolar environment when bound to the chaperone or when denatured in urea. These data suggested that PopB adopts a conformation more compact than that observed for molten globular PopD.[33]

PopB and PopD remain stably bound to PcrH in the bacterial cytoplasm in the absence of secretion, most likely to avoid protein aggregation and to maintain a secretion-competent conformation.[7,9] After the bacterium has contacted the target cell, PopB and PopD dissociate from PcrH and are

dx.doi.org/10.1021/bi200905x | *Biochemistry* 2011, 50, 7117−7131

presumably secreted through a narrow channel formed by the T3S needle (2−2.5 nm in diameter). Unfolded translocators are proposed to emerge from the tip of the T3S needle (formed by PcrV), in the proximity of the target membrane. PcrV is required to engage the membrane-inserted translocon with the T3S needle;[13,55,56] however, PcrV is not involved in the formation of the TM pore.[15] Therefore, the use of urea-isolated translocators to reconstitute membrane-inserted protein complexes is reasonable because the dilution of urea-isolated PopB and PopD in the presence of membranes likely resembles the in vivo translocon assembly process.

While negatively charged phospholipids are crucial for the binding of translocators to membranes and formation of TM pores in model membranes, cholesterol seems not to play a central role in vitro.[16] We tested how different lipids affected the pore formation properties of PopB and PopD in our experimental system. The presence of cholesterol and POPS in the liposomal membranes facilitated the insertion of the urea-isolated PopB and PopD (Figure 3). Other lipids like sphingomyelin and PE did not significantly alter the pore formation efficiency observed with POPC/POPS/cholesterol liposomes [65:15:20 molar ratio (data not shown)]. Therefore, we chose this composition as a simple and efficient model membrane system to study the assembly of PopB and PopD into lipid bilayers. Urea-isolated translocators formed discrete and stable pores in model membranes (Figures 4 and 5). Taken together, our data showed that the treatment with 6 M urea did not significantly alter the pore formation properties of the translocators.

We found that urea-isolated PopB, PopD, or an equimolar mixture of both translocators formed pores very similar to the pores formed when the translocators are dissociated from PcrH at acidic pH in the presence of membranes (Figure S3 of the Supporting Information). Interestingly, the comparison of both experimental systems suggested that acidic pH was required not only to dissociate the translocators from the chaperone (Figure S5 of the Supporting Information) but also to promote binding and insertion of translocators into membranes (Figures 4 and 6). We employed two independent experimental approaches, time-resolved FRET and sucrose-step gradient ultracentrifugation, to analyze the binding of the translocators to membranes at different pH values (Figure 6). Both assays clearly showed that binding at pH 4 was more efficient than at pH 6. Only a small fraction of the proteins was found associated with the membranes at pH 6. These results differ from those reported for the case in which heterogeneous aggregates of PopB and PopD were used.[16] The kinetic parameters used as a measure of membrane binding may represent the behavior of a small fraction of protein in the experimental system, and not necessarily the average behavior of all the protein in the sample (i.e., unbound protein does not generate a signal). Our data suggested that the decrease in the activity of the translocators at higher pH was, at least in part, caused by the inability of the proteins to bind to the lipid membrane.

A homogeneous sample is essential for the unambiguous interpretation of the spectroscopic signal obtained during the analysis of protein complexes assembled into membranes.[39] For this purpose, negatively charged phospholipids and low pH have been extensively used in the spectroscopic studies of pore-forming proteins like colicins, diphtheria toxin, Bcl-x_L, etc.[57−61] The requirement of acidic pH for the insertion of protein into membranes has been associated with the presence of acidic molten globular states.[62] While this pH-dependent conformational change may be relevant to the more compact PopB conformation (see above), PopD was found to have a molten globule conformation even at neutral pH.[33] Therefore, the spontaneous insertion of PopD (and/or PopB) segments into lipid bilayers may require the protonation of acidic residues, as shown before for bacteriorhodopsin fragments.[63] In our model system, the use of acidic pH maximized the assembly of discrete and stable TM pores. Such a low pH is presumably not encountered by the proteins when interacting with the plasma membrane of the target cell in vivo. Clearly, other still unidentified components present in the bacterium, or in the target cell, may facilitate the assembly of the translocon, but further studies are required in this area.

It has been widely assumed that assembled translocons contain both translocators forming a hetero-oligomer.[9] However, the structural arrangement of the membrane-inserted translocon and the stoichiometry of the complex are not known. By combining site-directed fluorescence labeling with both excitation energy migration and fluorescence quenching, we have shown that fluorescently labeled PopB interacted with native PopD in intact membrane-inserted complexes (Table 1). This interaction was confirmed by using the reverse combination of labeled PopD and native PopB. In both experiments, the intercalation of unlabeled molecules among the labeled ones produced the separation of the Bodipy dyes and consequently an increase in the fluorescence intensity, lifetime, and anisotropy of the sample. These results also implied that when added individually, both $PopD^{F223C-Bodipy}$ and $PopB^{S164C-Bodipy}$ formed homo-oligomers. Self-interaction of the translocators in intact membrane-inserted complexes was confirmed by the relative increase in the fluorescence intensity, lifetimes, and anisotropy of the sample when native PopD (or PopB) was mixed with $PopD^{F223C-Bodipy}$ (or $PopB^{S164C-Bodipy}$) and added to the membranes (data not shown).

In summary, we have established a cell-free system to analyze the structural assembly of the *P. aeruginosa* T3S translocators. Using this system, we found that PopB interacts with PopD when forming discrete and stable pores in intact membranes. Cell-free systems have been extremely useful for examining interactions among relevant protein components in membrane protein complexes and the study of their assembly and their structure (e.g., refs 44, 46, 57, 61, and 64−66). The identified mechanism and structural information obtained using the cell-free system are very valuable for the design of in vivo experiments and evaluation of the contribution of other known or unknown factors to the mechanism of T3S effector translocation.

■ ASSOCIATED CONTENT

Supporting Information

Details on cloning expression and purification of proteins, aggregation of the hisPcrH−PopB complex, PopB and PopD site-directed mutagenesis, SEC analysis of homogeneous chaperone−translocator complexes, pH dissociation vs urea dilution activities at pH 5.1, intermolecular disulfide formation by hisPcrH, pH solubility of the hisPcrH−PopD complex, steady-state FRET for protein−membrane binding, particle size analysis by DLS, and lifetime analysis for time-resolved FRET efficiencies. This material is available free of charge via the Internet at http://pubs.acs.org.

AUTHOR INFORMATION

Corresponding Author

*Address: 710 N. Pleasant St., Lederle GRT, Rm 816, University of Massachusetts, Amherst, MA 01003. Phone: (413) 545-2497. Fax: (413) 545-3291. E-mail: heuck@biochem.umass.edu.

Funding

This research was supported by a Biomedical Research Grant from the American Lung Association and the Massachusetts Thoracic Society to A.P.H. F.B.R. was partially supported by National Research Service Award T32 GM08515 from the National Institutes of Health. K.C.R. was a recipient of the Howard Hughes Medical Institute Undergraduate Science Program Summer Research Internship.

ACKNOWLEDGMENTS

We thank Prof. Carlos F. Gonzalez (Texas A&M University) for providing the *P. aeruginosa* PAO1 genomic DNA, Prof. Lila M. Gierasch for assistance with the CD measurements, Prof. Christopher Woodcock for his assistance with the initial transmission EM experiments, William Boston-Howes for the preliminary setup of the liposome flotation assay, Michael Buckner for the preparation of the $PopD^{F223C}$ mutant, and Sarah E. Kells for excellent technical assistance.

ABBREVIATIONS

Pop, *Pseudomonas* outer protein; Pcr, *Pseudomonas* low-calcium response; T3S, type III secretion; TM, transmembrane; IMAC, immobilized metal ion affinity chromatography; AEC, anion exchange chromatography; SEC, size exclusion chromatography; UV, ultraviolet; CD, circular dichroism; DLS, dynamic light scattering; POPC, 1-palmitoyl-2-oleoyl-*sn*-glycero-3-phosphocholine; POPE, 1-palmitoyl-2-oleoyl-*sn*-glycero-3-phosphoethanolamine; POPS, 1-palmitoyl-2-oleoyl-*sn*-glycero-3-phospho-L-serine; Fl, fluorescein; DTT, (2*S*,3*S*)-1,4-bis-sulfanylbutane-2,3-diol; EDTA, ethylenedinitrilotetraacetic acid; DPA, dipicolinic acid; HEPES, 2-[4-(2-hydroxyethyl)-piperazin-1-yl]ethanesulfonic acid; LB, Luria-Bertani; IPTG, isopropyl α-D-thiogalactopyranoside; Tris, 2-amino-2-(hydroxymethyl)propane-1,3-diol; FRET, Förster resonance energy transfer; SDS–PAGE, sodium dodecyl sulfate–polyacrylamide gel electrophoresis; Rh-PE, rhodamine B 1,2-dihexadecanoyl-*sn*-glycero-3-phosphoethanolamine; Bodipy, 4,4-difluoro-5,7-dimethyl-4-bora-3a,4a-diaza-3-indacene; PFO, Perfringolysin O.

REFERENCES

(1) Hueck, C. J. (1998) Type III protein secretion systems in bacterial pathogens of animals and plants. *Microbiol. Mol. Biol. Rev. 62*, 379–433.

(2) Galan, J. E., and Wolf-Watz, H. (2006) Protein delivery into eukaryotic cells by type III secretion machines. *Nature 444*, 567–573.

(3) Cornelis, G. R. (2006) The type III secretion injectisome. *Nat. Rev. Microbiol. 4*, 811–825.

(4) Frank, D. (1997) The exoenzyme S regulon of *Pseudomonas aeruginosa*. *Mol. Microbiol. 26*, 621–629.

(5) Hauser, A. R., Cobb, E., Bodi, M., Mariscal, D., Valles, J., Engel, J. N., and Rello, J. (2002) Type III protein secretion is associated with poor clinical outcomes in patients with ventilator-associated pneumonia caused by *Pseudomonas aeruginosa*. *Crit. Care Med. 30*, 521–528.

(6) Moraes, T. F., Spreter, T., and Strynadka, N. C. J. (2008) Piecing together the type III injectisome of bacterial pathogens. *Curr. Opin. Struct. Biol. 18*, 258–266.

(7) Mueller, C. A., Broz, P., and Cornelis, G. R. (2008) The type III secretion system tip complex and translocon. *Mol. Microbiol. 68*, 1085–1095.

(8) Buttner, D., and Bonas, U. (2002) Port of entry: The type III secretion translocon. *Trends Microbiol. 10*, 186–192.

(9) Mattei, P.-J., Faudry, E., Job, V., Izoré, T., Attree, I., and Dessen, A. (2011) Membrane targeting and pore formation by the type III secretion system translocon. *FEBS J. 278*, 414–426.

(10) Mueller, C.A., Broz, P., Muller, S. A., Ringler, P., Erne-Brand, F., Sorg, I., Kuhn, M., Engel, A., and Cornelis, G. R. (2005) The V-antigen of *Yersinia* forms a distinct structure at the tip of injectisome needles. *Science 310*, 674–676.

(11) Dacheux, D., Goure, J., Chabert, J., Usson, Y., and Attree, I. (2001) Pore-forming activity of type III system-secreted proteins leads to oncosis of *Pseudomonas aeruginosa*-infected macrophages. *Mol. Microbiol. 40*, 76–85.

(12) Sundin, C., Thelaus, J., Broms, J. E., and Forsberg, A. (2004) Polarisation of type III translocation by *Pseudomonas aeruginosa* requires PcrG, PcrV and PopN. *Microb. Pathog. 37*, 313–322.

(13) Goure, J., Pastor, A., Faudry, E., Chabert, J., Dessen, A., and Attree, I. (2004) The V antigen of *Pseudomonas aeruginosa* is required for assembly of the functional PopB/PopD translocation pore in host cell membranes. *Infect. Immun. 72*, 4741–4750.

(14) Vance, R. E., Rietsch, A., and Mekalanos, J. J. (2005) Role of the type III secreted exoenzymes S, T, and Y in systemic spread of *Pseudomonas aeruginosa* PAO1 *in vivo*. *Infect. Immun. 73*, 1706–1713.

(15) Schoehn, G., Di Guilmi, A. M., Lemaire, D., Attree, I., Weissenhorn, W., and Dessen, A. (2003) Oligomerization of type III secretion proteins PopB and PopD precedes pore formation in *Pseudomonas*. *EMBO J. 22*, 4957–4967.

(16) Faudry, E., Vernier, G., Neumann, E., Forge, V., and Attree, I. (2006) Synergistic pore formation by type III toxin translocators of *Pseudomonas aeruginosa*. *Biochemistry 45*, 8117–8123.

(17) Tardy, F., Homble, F., Neyt, C., Wattiez, R., Cornelis, G., Ruysschaert, J., and Cabiaux, V. (1999) *Yersinia enterocolitica* type III secretion-translocation system: Channel formation by secreted Yops. *EMBO J. 18*, 6793–6799.

(18) Hume, P. J., McGhie, E. J., Hayward, R. D., and Koronakis, V. (2003) The purified *Shigella* IpaB and *Salmonella* SipB translocators share biochemical properties and membrane topology. *Mol. Microbiol. 49*, 425–439.

(19) Pace, C. N., Vajdos, F., Fee, L., Grimsley, G., and Gray, T. (1995) How to measure and predict the molar absorption coefficient of a protein. *Protein Sci. 4*, 2411–2423.

(20) Moe, P. C., and Heuck, A. P. (2010) Phospholipid hydrolysis caused by *Clostridium perfringens* α-toxin facilitates the targeting of perfringolysin O to membrane bilayers. *Biochemistry 49*, 9498–9507.

(21) Shepard, L. A., Heuck, A. P., Hamman, B. D., Rossjohn, J., Parker, M. W., Ryan, K. R., Johnson, A. E., and Tweten, R. K. (1998) Identification of a membrane-spanning domain of the thiol-activated pore-forming toxin *Clostridium perfringens* perfringolysin O: An α-helical to β-sheet transition identified by fluorescence spectroscopy. *Biochemistry 37*, 14563–14574.

(22) Heuck, A. P., Tweten, R. K., and Johnson, A. E. (2003) Assembly and topography of the prepore complex in cholesterol-dependent cytolysins. *J. Biol. Chem. 278*, 31218–31225.

(23) Dalton, A. K., Murray, P. S., Murray, D., and Vogt, V. M. (2005) Biochemical characterization of Rous sarcoma virus MA protein interaction with membranes. *J. Virol. 79*, 6227–6238.

(24) Koppel, D. E. (1972) Analysis of macromolecular polydispersity in intensity correlation spectroscopy: The method of cumulants. *J. Chem. Phys. 57*, 4814–4820.

(25) Reinhart, G. D., Marzola, P., Jameson, D. M., and Gratton, E. (1991) A method for on-line background subtraction in frequency domain fluorometry. *J. Fluoresc. 1*, 153−162.

(26) Crowley, K. S., Liao, S., Worrell, V. E., Reinhart, G. D., and Johnson, A. E. (1994) Secretory proteins move through the endoplasmic reticulum membrane via an aqueous, gated pore. *Cell 78*, 461−471.

(27) vandeVen, M., Ameloot, M., Valeur, B., and Boens, N. (2005) Pitfalls and their remedies in time-resolved fluorescence spectroscopy and microscopy. *J. Fluoresc. 15*, 377−413.

(28) Boens, N., Qin, W., Basaric, N., Hofkens, J., Ameloot, M., Pouget, J., Lefevre, J. P., Valeur, B., Gratton, E., vandeVen, M., Silva, N. D., Engelborghs, Y., Willaert, K., Sillen, A., Rumbles, G., Phillips, D., Visser, A. J. W. G., vanHoek, A., Lakowicz, J. R., Malak, H., Gryczynski, I., Szabo, A. G., Krajcarski, D. T., Tamai, N., and Miura, A. (2007) Fluorescence lifetime standards for time and frequency domain fluorescence spectroscopy. *Anal. Chem. 79*, 2137−2149.

(29) Alcala, J. R., Gratton, E., and Prendergast, F. G. (1987) Resolvability of fluorescence lifetime distributions using phase fluorometry. *Biophys. J. 51*, 587−596.

(30) Wu, P. G., and Brand, L. (1994) Resonance energy transfer: Methods and applications. *Anal. Biochem. 218*, 1−13.

(31) Birket, S. E., Harrington, A. T., Espina, M., Smith, N. D., Terry, C. M., Darboe, N., Markham, A. P., Middaugh, C. R., Picking, W. L., and Picking, W. D. (2007) Preparation and characterization of translocator/chaperone complexes and their component proteins from *Shigella flexneri*. *Biochemistry 46*, 8128−8137.

(32) Tan, Y. W., Yu, H. B., Sivaraman, J., Leung, K. Y., and Mok, Y.-K. (2009) Mapping of the chaperone AcrH binding regions of translocators AopB and AopD and characterization of oligomeric and metastable AcrH-AopB-AopD complexes in the type III secretion system of *Aeromonas hydrophila*. *Protein Sci. 18*, 1724−1734.

(33) Faudry, E., Job, V., Dessen, A., Attree, I., and Forge, V. (2007) Type III secretion system translocator has a molten globule conformation both in its free and chaperone-bound forms. *FEBS J. 274*, 3601−3610.

(34) Job, V., Matteï, P.-J., Lemaire, D., Attree, I., and Dessen, A. (2010) Structural basis of chaperone recognition of type III secretion system minor translocator proteins. *J. Biol. Chem. 285*, 23224−23232.

(35) Manavalan, P., and Johnson, W. C. (1983) Sensitivity of circular dichroism to protein tertiary structure class. *Nature 305*, 831−832.

(36) Heuck, A. P., and Johnson, A. E. (2002) Pore-forming protein structure analysis in membranes using multiple independent fluorescence techniques. *Cell Biochem. Biophys. 36*, 89−101.

(37) Mutucumarana, V. P., Duffy, E. J., Lollar, P., and Johnson, A. E. (1992) The active site of factor IXa is located far above the membrane surface and its conformation is altered upon association with factor VIIIa. A fluorescence study. *J. Biol. Chem. 267*, 17012−17021.

(38) Hamman, B.D., Oleinikov, A. V., Jokhadze, G. G., Traut, R. R., and Jameson, D. M. (1996) Dimer/monomer equilibrium and domain separations of *Escherichia coli* ribosomal protein L7/L12. *Biochemistry 35*, 16680−16686.

(39) Johnson, A. E. (2005) Fluorescence approaches for determining protein conformations, interactions and mechanisms at membranes. *Traffic 6*, 1078−1092.

(40) Karolin, J., Johansson, L. B.-A., Strandberg, L., and Ny, T. (1994) Fluorescence and absorption spectroscopic properties of dipyrrometheneboron difluoride (Bodipy) derivatives in liquids, lipid membranes, and proteins. *J. Am. Chem. Soc. 116*, 7801−7806.

(41) Nicol, F., Nir, S., and Szoka, F. C. Jr. (1999) Orientation of the pore-forming peptide gala in POPC vesicles determined by a Bodipy-avidin/biotin binding assay. *Biophys. J. 76*, 2121−2141.

(42) Rosconi, M. P., Zhao, G., and London, E. (2004) Analyzing topography of membrane-inserted diphtheria toxin T domain using Bodipy-streptavidin: At low pH, helices 8 and 9 form a transmembrane hairpin but helices 5−7 form stable nonclassical inserted segments on the cis side of the bilayer. *Biochemistry 43*, 9127−9139.

(43) Bazzi, M. D., and Nelsestuen, G. L. (1987) Association of protein kinase C with phospholipid vesicles. *Biochemistry 26*, 115−122.

(44) Ramachandran, R., Tweten, R. K., and Johnson, A. E. (2005) The domains of a cholesterol-dependent cytolysin undergo a major FRET-detected rearrangement during pore formation. *Proc. Natl. Acad. Sci. U.S.A. 102*, 7139−7144.

(45) Posokhov, Y. O., and Ladokhin, A. S. (2006) Lifetime fluorescence method for determining membrane topology of proteins. *Anal. Biochem. 348*, 87−93.

(46) Lovell, J. F., Billen, L. P., Bindner, S., Shamas-Din, A., Fradin, C., Leber, B., and Andrews, D. W. (2008) Membrane binding by tBid initiates an ordered series of events culminating in membrane permeabilization by Bax. *Cell 135*, 1074−1084.

(47) Rivnay, B., and Metzger, H. (1983) Use of the airfuge for analysis and preparation of receptors incorporated into liposomes: Studies with the receptor for immunoglobulin E. *Anal. Biochem. 130*, 514−520.

(48) Bergstrom, F., Mikhalyov, I., Hagglof, P., Wortmann, R., Ny, T., and Johansson, L. B. A. (2002) Dimers of dipyrrometheneboron difluoride (Bodipy) with light spectroscopic applications in chemistry and biology. *J. Am. Chem. Soc. 124*, 196−204.

(49) Mikhalyov, I., Gretskaya, N., Bergström, F., and Johansson, L. B.-Å. (2002) Electronic ground and excited state properties of dipyrrometheneboron difluoride (Bodipy): Dimers with application to biosciences. *Phys. Chem. Chem. Phys. 4*, 5663−5670.

(50) Marushchak, D., Kalinin, S., Mikhalyov, I., Gretskaya, N., and Johansson, L. B.-Å. (2006) Pyrromethene dyes (Bodipy) can form ground state homo and hetero dimers: Photophysics and spectral properties. *Spectrochim. Acta, Part A 65*, 113−122.

(51) Heuck, A. P., Moe, P. C., and Johnson, B. B. (2010) The cholesterol-dependent cytolysins family of Gram-positive bacterial toxins. In *Cholesterol binding proteins and cholesterol transport* (Harris, J. R., Ed.) pp 551−577, Springer, New York.

(52) Czajkowsky, D. M., Hotze, E. M., Shao, Z., and Tweten, R. K. (2004) Vertical collapse of a cytolysin prepore moves its transmembrane β-hairpins to the membrane. *EMBO J. 23*, 3206−3215.

(53) Dang, T. X., Hotze, E. M., Rouiller, I., Tweten, R. K., and Wilson-Kubalek, E. M. (2005) Prepore to pore transition of a cholesterol-dependent cytolysin visualized by electron microscopy. *J. Struct. Biol. 150*, 100−108.

(54) Jameson, D. M., Croney, J. C., and Moens, P. D. (2003) Fluorescence: Basic concepts, practical aspects, and some anecdotes. *Methods Enzymol. 360*, 1−43.

(55) Sawa, T., Yahr, T. L., Ohara, M., Kurahashi, K., Gropper, M. A., Wiener-Kronish, J. P., and Frank, D. W. (1999) Active and passive immunization with the *Pseudomonas* V antigen protects against type III intoxication and lung injury. *Nat. Med. 5*, 392−398.

(56) Goure, J., Broz, P., Attree, O., Cornelis, G. R., and Attree, I. (2005) Protective anti-V antibodies inhibit *Pseudomonas* and *Yersinia* translocon assembly within host membranes. *J. Infect. Dis. 192*, 218−225.

(57) Wang, Y., Malenbaum, S. E., Kachel, K., Zhan, H., Collier, R. J., and London, E. (1997) Identification of shallow and deep membrane-penetrating forms of diphtheria toxin T domain that are regulated by protein concentration and bilayer width. *J. Biol. Chem. 272*, 25091−25098.

(58) Chenal, A., Savarin, P., Nizard, P., Guillain, F., Gillet, D., and Forge, V. (2002) Membrane protein insertion regulated by bringing electrostatic and hydrophobic interactions into play. A case study with the translocation domain of the diphtheria toxin. *J. Biol. Chem. 277*, 43425−43432.

(59) Thuduppathy, G. R., Terrones, O., Craig, J. W., Basanez, G., and Hill, R. B. (2006) The N-terminal domain of Bcl-x_L reversibly binds

membranes in a pH-dependent manner. *Biochemistry 45*, 14533−14542.

(60) Musse, A. A., Wang, J., deLeon, G. P., Prentice, G. A., London, E., and Merrill, A. R. (2006) Scanning the membrane-bound conformation of helix 1 in the colicin E1 channel domain by site-directed fluorescence labeling. *J. Biol. Chem. 281*, 885−895.

(61) Kyrychenko, A., Posokhov, Y. O., Rodnin, M. V., and Ladokhin, A. S. (2009) Kinetic intermediate reveals staggered pH-dependent transitions along the membrane insertion pathway of the diphtheria toxin T-domain. *Biochemistry 48*, 7584−7594.

(62) van der Goot, F. G., Gonzalez-Manas, J. M., Lakey, J. H., and Pattus, F. (1991) A 'molten-globule' membrane-insertion intermediate of the pore-forming domain of colicin A. *Nature 354*, 408−410.

(63) Hunt, J. F., Rath, P., Rothschild, K. J., and Engelman, D. M. (1997) Spontaneous, pH-dependent membrane insertion of a transbilayer α-helix. *Biochemistry 36*, 15177−15192.

(64) Shatursky, O., Heuck, A. P., Shepard, L. A., Rossjohn, J., Parker, M. W., Johnson, A. E., and Tweten, R. K. (1999) The mechanism of membrane insertion for a cholesterol-dependent cytolysin: A novel paradigm for pore-forming toxins. *Cell 99*, 293−299.

(65) Musse, A. A., and Merrill, A. R. (2003) The molecular basis for the pH-activation mechanism in the channel-forming bacterial colicin E1. *J. Biol. Chem. 278*, 24491−24499.

(66) Zakharov, S. D., Sharma, O., Zhalnina, M. V., and Cramer, W. A. (2008) Primary events in the colicin translocon: FRET analysis of colicin unfolding initiated by binding to BtuB and OmpF. *Biochemistry 47*, 12802−12809.